

Social deprivation and burden of influenza: Testing hypotheses and gaining insights from a simulation model for the spread of influenza



Ayaz Hyder^{a,*}, Brian Leung^{a,b}

^a Department of Biology, McGill University, Stewart Biology Building, 1205 ave Docteur Penfield, Montreal, QC, Canada H3A 1B1

^b School of Environment, McGill University, 3534 University St., Montreal, QC, Canada H3A 2A7

ARTICLE INFO

Article history:

Received 10 April 2014

Received in revised form 3 September 2014

Accepted 15 March 2015

Available online 21 March 2015

Keywords:

Influenza

Social inequalities

Vulnerable populations

Computer simulation

ABSTRACT

Factors associated with the burden of influenza among vulnerable populations have mainly been identified using statistical methodologies. Complex simulation models provide mechanistic explanations, in terms of spatial heterogeneity and contact rates, while controlling other factors and may be used to better understand statistical patterns and, ultimately, design optimal population-level interventions. We extended a sophisticated simulation model, which was applied to forecast epidemics and validated for predictive ability, to identify mechanisms for the empirical relationship between social deprivation and the burden of influenza. Our modeled scenarios and associated epidemic metrics systematically assessed whether neighborhood composition and/or spatial arrangement could qualitatively replicate this empirical relationship. We further used the model to determine consequences of local-scale heterogeneities on larger scale disease spread. Our findings indicated that both neighborhood composition and spatial arrangement were critical to qualitatively match the empirical relationship of interest. Also, when social deprivation was fully included in the model, we observed lower age-based attack rates and greater delay in epidemic peak week in the most socially deprived neighborhoods. Insights from simulation models complement current understandings from statistical-based association studies. Additional insights from our study are: (1) heterogeneous spatial arrangement of neighborhoods is a necessary condition for simulating observed disparities in the burden of influenza and (2) unmeasured factors may lead to a better quantitative match between simulated and observed rate ratio in the burden of influenza between the most and least socially deprived populations.

© 2015 The Authors. Published by Elsevier B.V. This is an open access article under the CC BY-NC-ND license (<http://creativecommons.org/licenses/by-nc-nd/4.0/>).

1. Introduction

Seasonal influenza epidemics pose several challenges for society in terms of social, economic and health impacts (Molinari et al., 2007). These impacts are not always proportional among different populations. Lower vaccination coverage may increase susceptibility to infection in some racial/ethnic groups (Lu et al., 2013). Heterogeneous contact patterns due to social and demographic factors may affect disease transmission between populations (Charland et al., 2011; Laskowski et al., 2011; Mossong et al., 2008). Also, material/social deprivation, neighborhood socioeconomic status, distrust of authority, and access to health care services may be driving disparities in the burden of influenza

(Charland et al., 2011; Crighton et al., 2007; Loeb, 2003; Principi et al., 2003).

Social determinants of health, such as social deprivation, are inherently constructs of individual- and neighborhood-level factors. In Charland et al. (2011), social deprivation, which represented social support, cohesion and cooperation at the neighborhood scale, was negatively associated with the burden of influenza. Specifically, social deprivation reflected family-type composition within households (e.g., living alone and single-parent families). Household characteristics, such as size, structure, and presence of school-aged children, affect disease transmission and severity via differences in susceptibility and contact patterns (Cauchemez et al., 2009; House and Keeling, 2009; Longini et al., 1982; Marathe et al., 2011; Stroud et al., 2007). Despite these past findings, the combined role of family-type composition and spatial heterogeneity of neighborhoods with dissimilar distribution of family-type households has not been studied as a possible explanation for the relationship between social deprivation and burden of influenza, as reported in Charland et al. (2011).

* Corresponding author. Present address: Dalla Lana School of Public Health, University of Toronto, 155 College Street, 6th Floor, Toronto, ON, Canada M5T 3M7. Tel.: +1 416 978 2201; fax: +1 416 978 8299.

E-mail address: ayaz.hyder@utoronto.ca (A. Hyder).

While current statistical models have identified interesting patterns between social deprivation and the burden of influenza (Charland et al., 2011), complementary methodologies, which explicitly consider the outcome of putative mechanisms, may be useful to explore (Auchincloss and Diez Roux, 2008). Particularly, individual-based models (IBMs), which are also called agent-based models, offer a unique way to model real-world processes and have extensively been used to model the spatial spread of influenza (degli Atti et al., 2008; Eubank et al., 2004; Ferguson et al., 2005; Germann et al., 2006). In an IBM, interactions are modeled between agents (e.g., people), their characteristics (e.g., age, pre-existing immunity, place membership at school or work) and processes (e.g., infectiousness over time, place-based contact probabilities, staying home from work/school). IBMs offer flexibility in modeling nonlinear, dynamic, and feedback processes over multiple spatial and temporal scales (Auchincloss and Diez Roux, 2008; Galea et al., 2010; Mabry et al., 2008). Importantly, these IBMs will allow us to ask whether we can understand the observed effects of social deprivation mechanistically in terms of spatial heterogeneity, contact rates, etc. Conversely, we can examine whether the rich theoretical developments on IBMs of the spread of influenza is consistent with and sufficient to explain observed patterns of social deprivation and burden of influenza. Ultimately, the IBM is a virtual platform that leverages detailed information on individual-, household- and neighborhood-level factors to design, test and predict the impact of novel mitigation strategies.

With this in mind, we propose to use and extend a sophisticated simulation model, which has been developed and applied to forecast epidemics as well as validated for predictive ability (Hyder et al., 2013), to examine mechanistically the observed relationship between social deprivation and the burden of influenza. We hypothesize that the influence of social deprivation on the burden of influenza is mediated through the distribution of household size and contact patterns. In the context of social deprivation, our conceptualization of household size includes data on family type or structure, such as living alone, as a couple with no kids or parent(s) with one or more child. Due to spatial heterogeneity in social deprivation, we also hypothesize that the spatial arrangement of households of different size (due to family type) may affect epidemic dynamics at larger (city) and local (neighborhood) spatial scales.

2. Methods

2.1. Simulation model

Our model was a spatially-explicit stochastic representation of influenza epidemics in the Census Metropolitan Area of Montreal (CMA). We used census data to recreate key demographic and contact patterns, such as age and household size distribution, place membership (e.g. number of employees in a workplace and number of students in each grade level), age-based contact within households, schools and workplaces and random contact in the community. Disease natural history parameters, such as latent period, infectiousness profile and recovery, were modeled based on probabilistic functions using literature-based parameters. Disease transmission was modeled by calculating a force of infection due to infectious contact with infected individuals from three sources: household, place (school or workplace) and community. We calibrated transmission coefficients for each of these three sources using observed data on the: (i) laboratory surveillance data and (ii) age-based clinical attack rates. Details on model formulation, mathematical equations, and data sources schools and workplaces are found in the Supplementary material while details about households are given below. Further details of model fitting,

calibration and validation may be found elsewhere (Hyder et al., 2013).

We used the Public Use Microdata File (Households) from Statistics Canada (Statistics Canada, 2005) to model household characteristics (e.g., size, family-type) and the age distribution of individuals within households. We considered four family types: two parents with children, one parent with children, couples without kids, and individuals living alone. Note that these households may contain other individuals than just parents, couples and kids. Related to social deprivation, neighborhoods in our model were defined by census tract boundaries based on the 2001 Census conducted by Statistics Canada.

2.2. Model scenarios

We used this IBM to simulate epidemics under scenarios that differed in family-type composition and spatial arrangement. We hypothesized the interaction of these two mechanisms as the primary drivers of the observed relationship between social deprivation and burden of influenza. In our three scenarios (see below), family-type composition within neighborhoods was set to random or heterogeneous and spatial arrangement between neighborhoods' social deprivation level was set to random or "empirical" heterogeneous "Empirical" here implied that we used the observed distribution of social deprivation level in the study area (Fig. 1) (Institut National de Sante Publique du Quebec, 2001).

Scenario 1: random neighborhood composition and spatial location.

Scenario 2: heterogeneous neighborhood composition and random spatial arrangement of neighborhoods.

Scenario 3: heterogeneous neighborhood composition and "empirical" heterogeneous spatial arrangement of neighborhoods.

To model scenario 1, we randomly distributed households across neighborhoods while matching the observed number of individuals within each neighborhood. Thus, we controlled for neighborhood size, but composition and spatial arrangement were random. We labeled this the "Null model" since it did not consider any information of social deprivation, and was analogous to the general formulations of influenza IBMs.

To model scenario 2, we collected data on social deprivation index (SDI) (Institut National de Sante Publique du Quebec, 2001) and the proportion of different family types for each neighborhood. SDI values of 1 (lowest) to 5 (highest) represented levels of social deprivation. For neighborhoods with missing SDI values, we assigned average values from adjacent neighborhoods. In combination, these data provided a list of neighborhoods indicating their SDI value and the proportion of households of each family-type. Using this list, we randomly assigned each neighborhood a SDI value and the corresponding family-type distribution. We used the assigned family-type distribution to distribute households within neighborhoods. In this way, we removed any spatial heterogeneity in SDI values but retained the realistic (and heterogeneous) distribution of household size and family type according to the assigned SDI value. We labeled this the "Composition model" because it modeled the realistic family-type composition within neighborhoods.

In scenario 3, we used the observed SDI value for each neighborhood and then distributed households. This allowed us to match the observed and simulated data within each neighborhood in terms of their: (i) composition, as measured by the proportion of households of each family type, and (ii) spatial location, as measured by the spatial arrangement of social deprivation levels. We labeled this the "full SDI model".

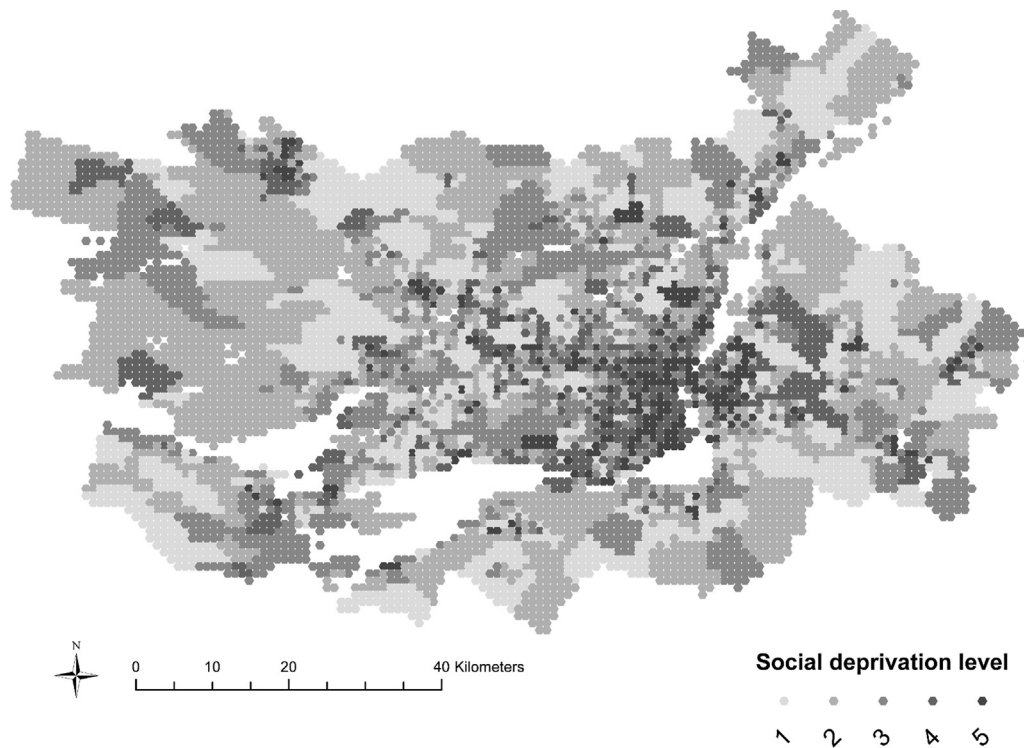


Fig. 1. Map of the study area (Census Metropolitan Area of Montreal). Each point represents a grid cell in the model. The color of the dot represents the level of social deprivation (darker colors mean higher social deprivation) based on empirical data from the Canada census conducted by Statistics Canada.

We fitted each model scenario to observed data from a past influenza epidemic (1998–1999 influenza season). Models were fitted under the assumption of 100 initial infections that were randomly selected from the entire population with the requirement that the infected person must reside in a grid cell with a total population of 100 or more people. These assumptions for initial conditions ensured that epidemics were not too slow or too fast and that epidemics did not die out too quickly. We varied these two assumptions about location and number of initial in a sensitivity analysis (see below). We assumed pre-existing immunity and vaccination in the population. For pre-existing immunity, we scaled the force of infection among vaccinated individuals by 0.25. In all simulations, we assumed 15% of infants (0–2 years old), 12% of kids (3–18 years old), 8% of adults (19–64 years old) and 44% of seniors (65 years and older) were vaccinated with vaccine effectiveness values (age groups) of: 0% (for 0–2 years), 50% (for 3–64 years) and 20% (for 65 years and over). Further details on model fitting and initial conditions have been described in Hyder et al. (2013). We simulated 50 epidemics for each modeled scenario and calculated various epidemic metrics for each modeled scenario as the average across all simulated epidemics. This number of simulations was reasonable because of the intensive computational resources required for each run of the model, the number of model scenarios in our study, and the amount of data that we needed to record and process for calculating epidemic metrics (see below) by type of neighborhood and age group.

2.3. Epidemic metrics

We calculated two epidemic metrics: age-based attack rate (AR) and epidemic timing. We assumed that attack rate was a proxy indicator of burden of influenza. In reality, influenza burden was a function of several factors including age, co-morbidities, severity of infection and other factors related to healthcare-seeking behavior. Due to these complexities and the use of influenza-like-illness (ILI)

data to broadly track the actual number of influenza cases in the population (Cooley et al., 2008), we believe this was a reasonable assumption.

To understand the overall or city-wide difference in burden of influenza between modeled scenarios we plotted the mean AR with 95% confidence intervals (CI) for each age group: 0–5, 6–17, 18–24, 25–44, 45–64, 65–74, 75–84, 85 and over. At the neighborhood scale, we also plotted epidemic metrics (AR and peak week) against the social deprivation index. In these latter plots, AR was calculated for each age group within each neighborhood and then averaged across all neighborhoods based on their SDI. We used the epidemic curve for each age group within each neighborhood to calculate peak week. We averaged these peak week values across all neighborhoods with the same level of social deprivation to plot the relationship between peak week and SDI by age group. We also included a best-fit regression line to determine if there was any difference in this relationship between modeled scenarios. We performed calculations for AR and peak week by age group in order to control for confounding in the SDI–influenza burden relationship by age-related factors, such as contact rates and pre-existing immunity.

2.4. Sensitivity analysis

We performed the following analysis to test the sensitivity of two relationships: (1) overall attack rate and model scenario by age group and (2) social deprivation level of neighborhood and burden of influenza by age group. We mainly tested the robustness of our results under the Full SDI model scenario because this was the scenario that we hypothesized would explain the empirical relationship between social deprivation and burden of influenza. If our results were sensitive, then factors other than the ones we have proposed under the Full SDI model scenario – neighborhood composition and spatial arrangement of neighborhoods – may have explained the empirical relationship.

To explore this further, we performed univariate sensitivity analysis for: (i) location of initial infections, (ii) number of initial infections, (iii) effect of increased mixing and (iv) level of disease transmission. For location of initial infections, we assumed two alternative seeding scenarios where only neighborhoods with the lowest or highest level of social deprivation, labeled as Low SDI and High SDI neighborhoods, were seeded with initial infections. Our main results were based on randomly selecting neighborhoods regardless of level of social deprivation. In a separate analysis, we varied the number of initial infections, which was set to 50, 100 (assumed for main results) or 150. Apart from these analysis for initial conditions, we also varied model parameters and assumptions related to contact structure and disease transmission.

Our main results assumed age-dependent random community contacts (see Supplementary material). This was an important sensitivity to test because the number and age of parents, children and other household members determined the family type structure. Consequently, it was likely that spatial proximity to community contacts of a certain age was also influenced under the Full SDI model scenario. To test the influence of age-based contact on our results, we simulated epidemics with age-independent random community contact. Mathematically, we set the value to 1 for all age groups in the model parameter that scaled the force of infection due to community contacts, $\zeta(a_i)$ in Eq. (1) of the Supplementary material. In our main results we assumed different values for $\zeta(a_i)$ based on an individual's age group (see Supplementary material).

Our last sensitivity analysis varied the level of disease transmission in the model. The proportion of disease transmission, which occurred in households, schools, workplaces and community, was calibrated to match: (i) age-based clinical attack rates reported in the literature for influenza epidemics and (ii) the observed data from 1998 to 1999 influenza epidemic in our study area. Therefore, we varied the overall level of disease transmission while maintaining the calibrated values for proportion of disease transmission by varying the model parameter β_{constant} , which scaled the overall level of transmission (see Supplementary material). Since our main results were generated with $\beta_{\text{constant}} = 1.65$, we varied it by ± 0.5 to model higher or lower levels of disease transmission. Varying this critical model parameter likely translated into different values of the basic reproduction number R_0 , which was the average number of secondary infections due to a single initial infection in a completely susceptible population, although we did not actually measure the value of R_0 .

3. Results

There was considerable spatial variation of SDI in CMA Montreal (Fig. 1). High social deprivation was mainly concentrated in the downtown and east part of Montreal Island. In contrast, most suburban and rural areas showed low social deprivation. All models matched the observed epidemic of 1998–1999 well, in terms of peak week, duration of the epidemic, and absolute intensity (Fig. 2a and b). As expected, household size distribution within neighborhoods varied with the level of social deprivation (results not shown). For example, average proportion of the living alone household type was 24% and 7% in neighborhoods with high (SDI = 5) and low (SDI = 1) social deprivation, respectively.

For the overall AR, we observed some differences between models (Fig. 3). Consistently across age groups, except 85 years and over, AR differed between the Null and full SDI model. On average, the absolute difference in AR between the Null and full SDI model was less than 0.5. For the Composition model, there was no consistent pattern because, depending on the age group, AR was closer to either of the other models.

In the Null model, SDI and AR were not related for all age groups (Fig. 4). In comparison, the negative relationship between SDI and AR was clearly apparent across all age groups in the full SDI model. In this scenario, the difference in AR between the least and most socially deprived neighborhoods was as little as $\sim 0.75\%$ in the 6–17 years old group and as high as $\sim 2.5\%$ in other age groups (e.g., 18–24 and 25–44 years old). The SDI–AR relationship under the Composition model was closer to the Null model than the full SDI model.

With regards to peak week, we observed a positive relationship between SDI and peak week, irrespective of the modeled scenario (Fig. 5). The difference in peak week between the least and most socially deprived neighborhoods was greater in the full SDI model than other scenario. Furthermore, we observed a steeper regression line for the SDI–peak week relationship among most age groups under the full SDI model.

Overall, our main results were robust to various sensitivity analyses. Under different assumptions and values for location and number of initial infections, we did not observe major deviations in our main results, which included the relationship between overall AR by age group and the relationship between SDI and AR by age group (Figs. S1–S4). On the other hand, changes in contact structure and level disease transmission quantitatively changed the results but not qualitatively. For contact structure, we observed a higher overall AR by age group under the assumption of age-independent random community contacts (Fig. S5) but no change in the direction of the relationship between AR and SDI by age group (Fig. S6). We observed similar results when we varied levels of disease transmission. Higher or lower disease transmission relative to the level of transmission that was fitted to an observed epidemic increased (Fig. S7) or decreased (Fig. S9) the overall AR by age group, respectively. Consequently, the SDI–AR relationship was vertically shifted toward higher or lower AR values but there was no change in the direction of the relationship across age groups, which remained negative in line with our main results (Figs. S8 and S10).

4. Discussion

Previous studies have used statistical methods to describe empirical relationships between the burden of influenza and social determinants of health (Charland et al., 2011; Crighton et al., 2007). We used a simulation model to further explain one such relationship—higher social deprivation is associated with lower burden of influenza. Furthermore, we explored the larger ramifications of social deprivation on disease spread and its patterns (e.g., age-based attack rates and epidemic timing).

Our main finding was that there was a greater variability in attack rates and peak week between the most and least socially deprived neighborhoods under the full SDI model than other modeled scenarios. Our use of multiple model scenarios allowed us to systematically show that neighborhood composition or spatial arrangement alone were not sufficient to explain the observed relationship between social deprivation and burden of influenza. Beyond this, our findings also highlighted important consequences of social deprivation on patterns at multiple spatial scales.

Specifically, we found that spatial arrangement of neighborhoods was critical to the influence of local-scale heterogeneities in neighborhood composition on larger-scale epidemic patterns between neighborhoods. For example, we observed a greater lag in epidemic peak week between the least and most socially deprived neighborhoods under the full SDI model than the Composition model. The only difference between these two models was the spatial arrangement of neighborhoods. One inference from this finding is that spatial heterogeneity in social deprivation levels may strongly couple epidemic dynamics between adjacent

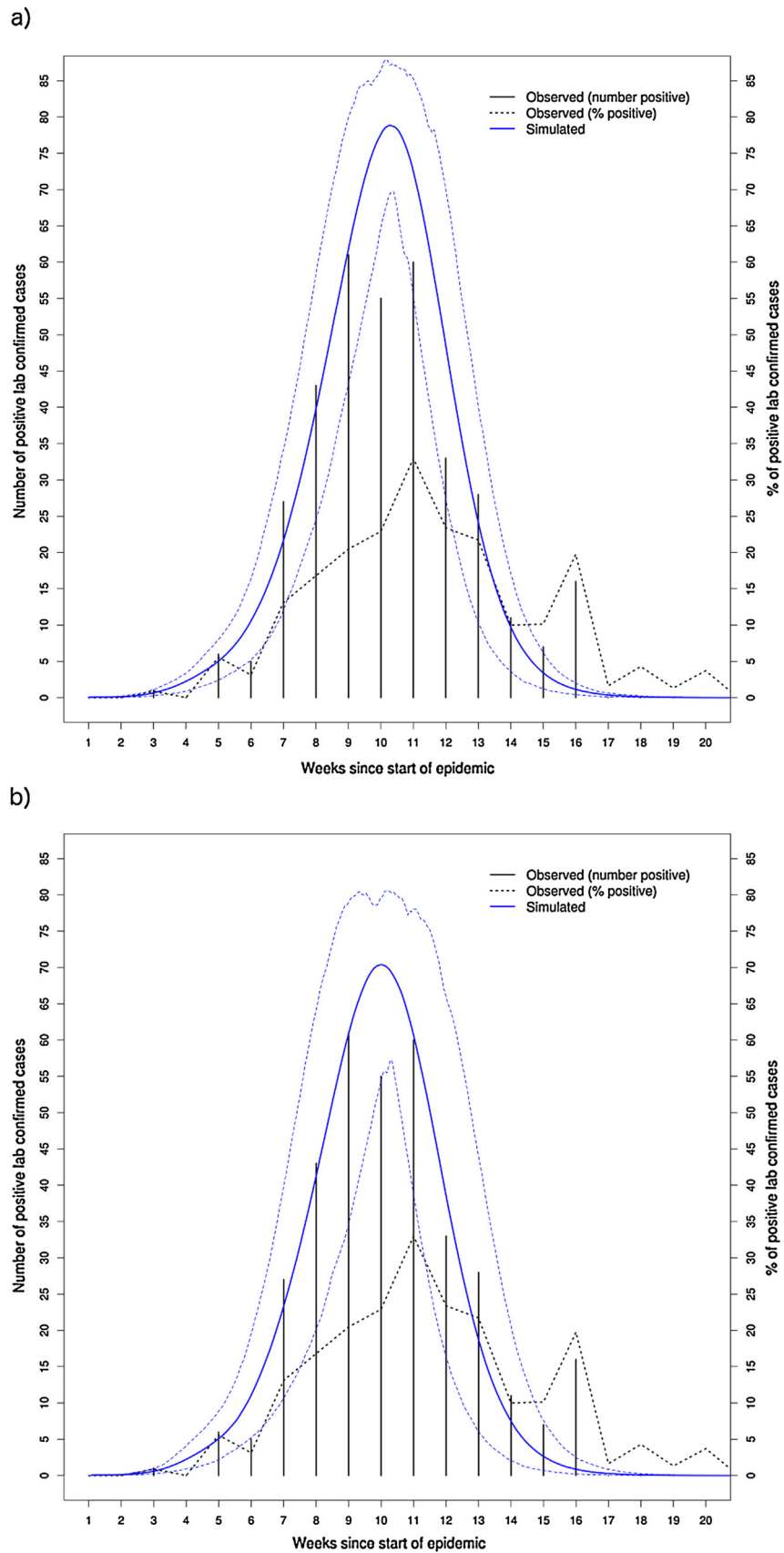


Fig. 2. Fit of simulated epidemics to observed data. (a) Full SDI model and (b) Null model. Solid continuous (blue) line represents average epidemic curve (from simulated epidemics) and dotted continuous (blue) lines represent upper and lower 95% confidence intervals. Dotted (black) line is percentage of viral samples that were positive for influenza and solid (black) height bars represent the number of viral samples that were positive for influenza based on laboratory surveillance data collected during the 1998–1999 influenza season in the Census Metropolitan Area of Montreal, Quebec, Canada. (For interpretation of the references to color in this figure legend, the reader is referred to the web version of this article.)

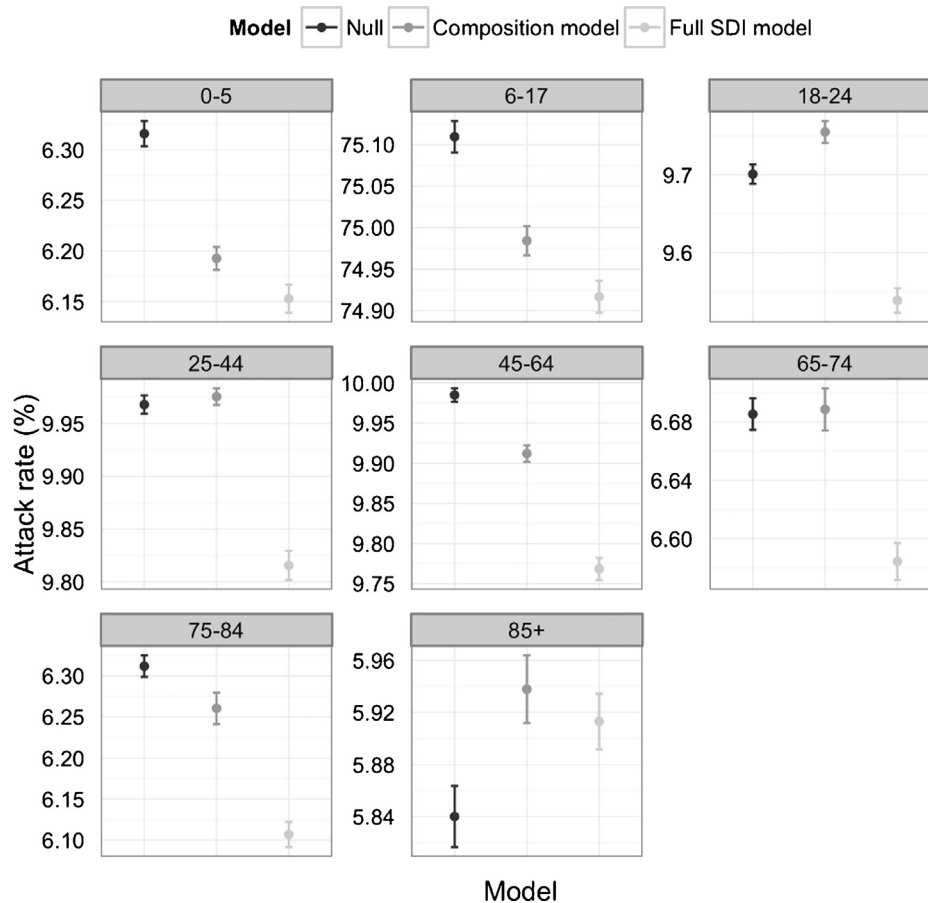


Fig. 3. Overall (city-wide) attack rate by age group and model scenario (see main text for details). Solid dots represent the average attack rate while upper and lower bars represent 95% confidence intervals around each mean.

neighborhoods. Such coupling has been demonstrated in metapopulation models for infectious diseases where it was shown that correlation in epidemic dynamics between two populations was dependent on the strength of their coupling, regardless of population size (Keeling and Rohani, 2002). Another inference is that even if neighborhood composition was heterogeneous (as in the Composition model), it was not sufficient to lead to variability at larger spatial scales. This may have been the case because disease spread at the city scale is too fast or the level of heterogeneity in households due to family size was not sufficiently large enough to allow for any effect of local scale heterogeneities on larger scale patterns.

Our study findings and their subsequent inferences suggest that it may be optimal to target non-pharmaceutical interventions for mitigating burden of influenza at neighborhoods that are characterized by: low social deprivation and clustered in space. Such a strategy may be optimal because it may slow down disease spread among households with generally more school-aged children where those children may be attending similar schools due to their spatial proximity. This is a novel strategy because it takes advantage of the underlying sociodemographic profile of neighborhoods and uses it to try to slow down disease spread. There is some evidence from the literature that, when taken together with our findings, support further exploring such a mitigation strategy. For example, although we did not look at household size directly, previous studies found associations between household size and (1) the probability of disease transmission (House et al., 2012) and (2) burden of influenza (Stroud et al., 2007). Also, other studies have highlighted an association between presence of dependent children and epidemic severity (House and Keeling, 2009) a role for family structure on the burden of influenza (Kimura et al., 2011).

Since this study was motivated by the empirical relationship between social deprivation and burden of influenza, it is useful to compare our results with those reported in Charland et al. (2011). Although not directly comparable to the rate ratio based on healthcare utilization rates for influenza between the most and least socially deprived neighborhoods, which was 0.21 in Charland et al. (2011), the rate ratio calculated similarly but based on attack rates was approximately 0.82 in our study. This would suggest that while neighborhood composition and spatial arrangement definitely contributed to the observed patterns and the simulated contact patterns were in the correct direction, these factors did not fully explain the observations. Some reasons for our higher rate ratio was that we did not account for other factors related to seeking healthcare services, such as co-morbidity and socioeconomic status, and we included a larger study area (CMA Montreal) whereas in Charland et al. (2011) only the City of Montreal was included in the analysis.

Our results were only quantitatively modified under two sensitivity analyses in which we varied assumptions regarding contact structure and level of disease transmission. Despite this, our study's main result – the negative relationship between social deprivation and burden of influenza – was consistently observed under all sensitivity analyses. Level of disease transmission and contact structure are key parameters in the spread of influenza and, therefore, it was not surprising that higher transmission or age-independent contact structure increased the overall and neighborhood-level attack rate by age group. Although, we did not perform sensitivity analyses to the same extent for other model scenarios (Null and Composition model), we expected to observe similar results as those reported for the Full SDI model

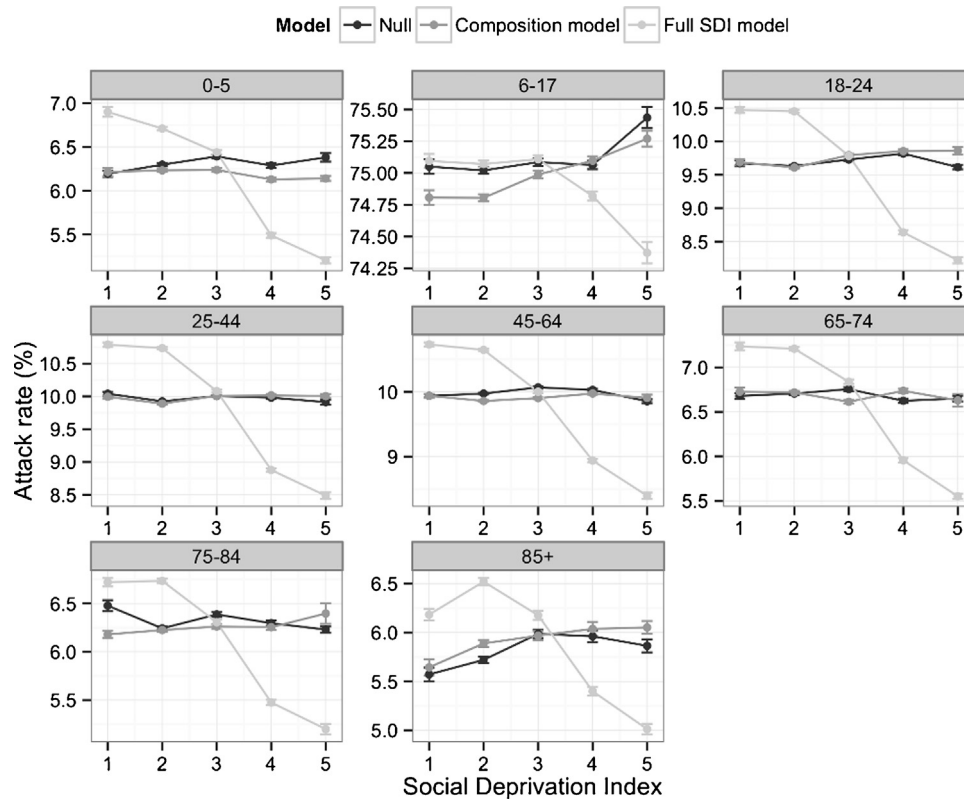


Fig. 4. Neighborhood-level attack rate by social deprivation index of neighborhood, age group and model scenario. Higher value of Social Deprivation Index represents greater level of neighborhood-level social deprivation. Dots represent the average attack rate while upper and lower bars represent 95% confidence intervals.

scenario. This was expected because changing the number of initially infected individuals or the location of initial infections did not lead to significant structural changes in the model or epidemic dynamics. As a result, quantitative differences in the overall AR across all age groups (Figs. S1–S4) were very small and when differences did occur they were in very specific age groups (e.g., 6–17 years old or 85 years and over). For variations in disease transmission and contact structure, we expected consequences for epidemic dynamics at larger spatial scales because of the manner in which we formulated the model. Increased levels of overall disease transmission amplified the force of infection between individuals without affecting transmission dynamics since we maintained the proportion of disease transmission between sources of contact (e.g., household, schools). Therefore, we observed quantitative differences due to changes in overall intensity and speed of the epidemic rather than qualitative differences. Similarly, assuming age-independent contact structure increased the individual force of infection but only slightly given the lower levels of transmission we assumed due to community contacts. Future work on this model could explicitly model more detailed contact processes between households, schools, workplaces and community, to determine how local scale changes in social contacts may affect the relationship between social deprivation and burden of influenza. Examples of such detailed contact processes may include network of networks (Gonzalez and Barabasi, 2007) or urban transportation systems (Eubank et al., 2004).

There were some limitations in our study. We assumed that census tracts approximated neighborhoods whereas the neighborhood was represented by dissemination area—a smaller spatial unit in Charland et al. (2011). This limitation may have weakened the relationship between social deprivation and burden of influenza because we essentially averaged over several smaller spatial units.

This limitation was difficult to overcome because the census data that we used to formulate households was only available at the census tract level. Another limitation was the uncertainty in parameters, initial conditions and assumptions of the underlying IBM that we used in this study. Although we performed univariate sensitivity analysis for some initial conditions and model parameters, multivariate sensitivity analyses for all model parameters may further inform the robustness of our findings. For the parameters that we did attempt to vary and generate results for, we did not observe any consistent patterns that would lead us to conclude anything different than our stated findings and inferences.

We concluded that the negative relationship between social deprivation and the burden of influenza might be due to neighborhood composition, which may have modified local-scale contact processes, and spatial arrangement, which provided mechanism to couple local-scale epidemic dynamics resulting in larger scale patterns. To the best of our knowledge, these two factors have not been simultaneously considered in previous modeling studies (House and Keeling, 2009; Laskowski et al., 2011; Marathe et al., 2011). Between the Null and Composition model, we found no differences in epidemic metrics due to changes only in neighborhood composition. Between the Composition and Null model, we showed the importance of spatial arrangement on qualitatively replicating the empirical relationship between social deprivation and burden of influenza. Given the annual cycle of influenza epidemics, existing disparities in the burden of influenza due to social deprivation may be effectively reduced if public health interventions and programs were to consider the joint influence of both factors that we have identified in our study. Complex simulation models, such as the one we utilized in our study, can assist in identifying, testing and fine-tuning mitigation strategies that are optimal, practical, and cost-effective.

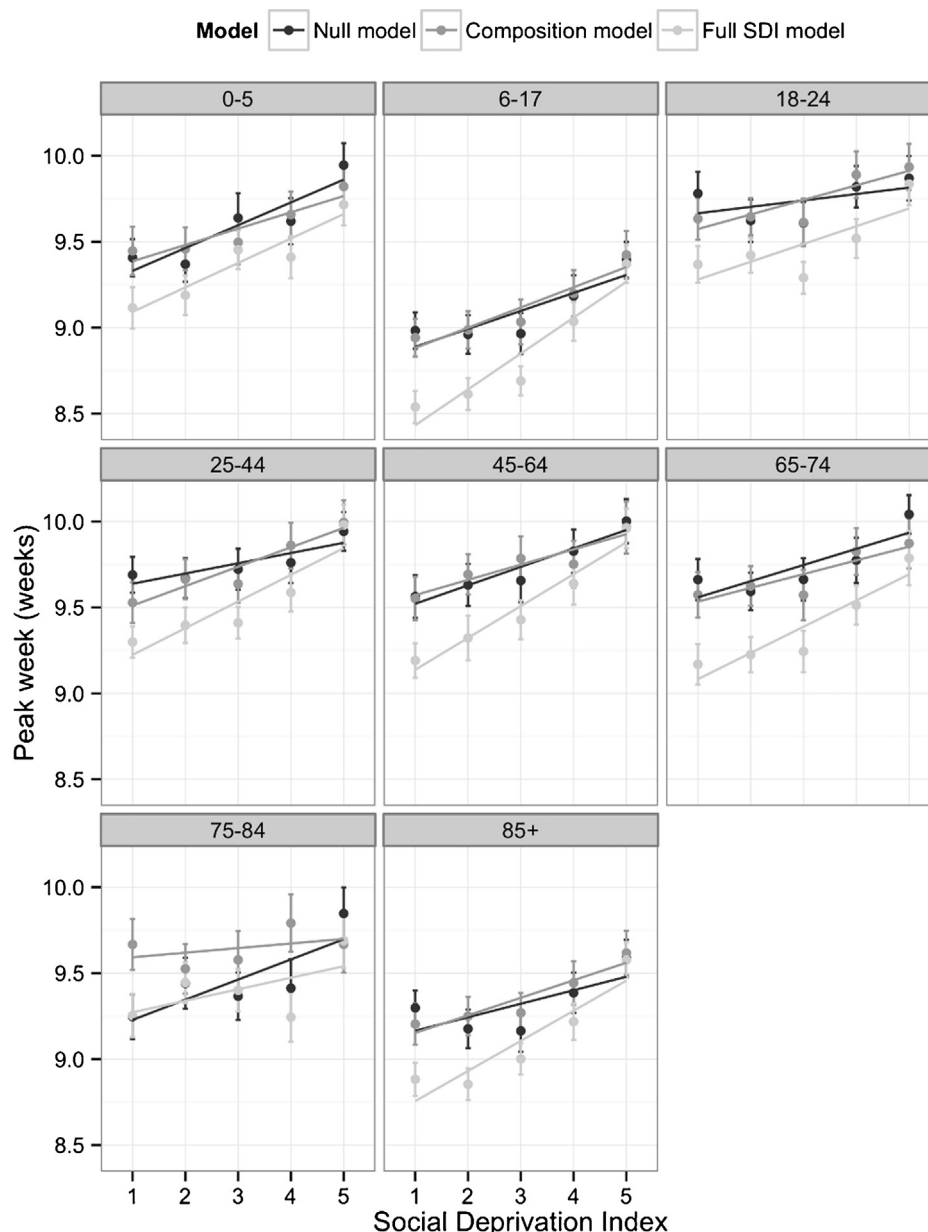


Fig. 5. Neighborhood-level epidemic peak week by social deprivation index of neighborhood, age group and model scenario. Dots represent the average peak week while upper and lower bars represent 95% confidence. Lines represent best-fit regression model for each modeled scenario based on average peak week within each panel. Peak week was based on epidemic curves constructed for each age group within neighborhoods and then averaged across neighborhoods with the same social deprivation index. Higher value of Social Deprivation Index represents greater level of neighborhood-level social deprivation.

Conflict of interest statement

The authors declare there is no conflict of interest.

Appendix A. Supplementary data

Supplementary data associated with this article can be found, in the online version, at [doi:10.1016/j.epidem.2015.03.004](https://doi.org/10.1016/j.epidem.2015.03.004).

References

- Auchincloss, A.H., Diez Roux, A.V., 2008. A new tool for epidemiology: the usefulness of dynamic-agent models in understanding place effects on health. *Am. J. Epidemiol.* 168, 1–8.
- Cauchemez, S., Donnelly, C.A., Reed, C., Ghani, A.C., Fraser, C., Kent, C.K., Finelli, L., Ferguson, N.M., 2009. Household transmission of 2009 pandemic influenza A (H1N1) virus in the United States. *N. Engl. J. Med.* 361, 2619–2627.
- Charland, K.M., Brownstein, J.S., Verma, A., Brien, S., Buckridge, D.L., 2011. Socio-economic disparities in the burden of seasonal influenza: the effect of social and material deprivation on rates of influenza infection. *PLoS ONE*, 6.
- Cooley, P., Ganapathi, L., Ghneim, G., Holmberg, S., Wheaton, W., Hollingsworth, C.R., 2008. Using influenza-like illness data to reconstruct an influenza outbreak. *Math. Comput. Model.* 48, 929–939.
- Crighton, E.J., Elliott, S.J., Moineddin, R., Kanaroglou, P., Upshur, R., 2007. A spatial analysis of the determinants of pneumonia and influenza hospitalizations in Ontario (1992–2001). *Soc. Sci. Med.* 64, 1636–1650.
- degli Atti, M.L.C., Merler, S., Rizzo, C., Ajelli, M., Massari, M., Manfredi, P., Furlanello, C., Tomba, G.S., Iannelli, M., 2008. Mitigation measures for pandemic influenza in Italy: an individual based model considering different scenarios. *PLoS ONE* 3 (3), e1790.
- Eubank, S., Guclu, H., Kumar, V.S.A., Marathe, M.V., Srinivasan, A., Toroczkai, Z., Wang, N., 2004. Modelling disease outbreaks in realistic urban social networks. *Nature* 429, 180–184.
- Ferguson, N.M., Cummings, D.A.T., Cauchemez, S., Fraser, C., Riley, S., Meeyai, A., Iam-sirithaworn, S., Burke, D.S., 2005. Strategies for containing an emerging influenza pandemic in Southeast Asia. *Nature* 437, 209–214.

- Galea, S., Riddle, M., Kaplan, G.A., 2010. Causal thinking and complex system approaches in epidemiology. *Int. J. Epidemiol.* 39, 97–106.
- Germann, T.C., Kadau, K., Longini Jr., I.M., Macken, C.A., 2006. Mitigation strategies for pandemic influenza in the United States. *Proc. Natl. Acad. Sci. U.S.A.* 103, 5935–5940.
- Gonzalez, M.C., Barabasi, A.-L., 2007. Complex networks: from data to models. *Nat. Phys.* 3, 224–225.
- House, T., Inglis, N., Ross, J.V., Wilson, F., Suleman, S., Edeghere, O., Smith, G., Olowokure, B., Keeling, M.J., 2012. Estimation of outbreak severity and transmissibility: influenza A(H1N1)pdm09 in households. *BMC Med.* 10, 117.
- House, T., Keeling, M.J., 2009. Household structure and infectious disease transmission. *Epidemiol. Infect.* 137, 654–661.
- Hyder, A., Buckeridge, D.L., Leung, B., 2013. Predictive validation of an influenza spread model. *PLoS ONE* 8, e65459.
- Institut National de Sante Publique du Quebec, 2001. Deprivation Index for Health in Canada. Institut National de Sante Publique du Quebec.
- Keeling, M.J., Rohani, P., 2002. Estimating spatial coupling in epidemiological systems: a mechanistic approach. *Ecol. Lett.* 5, 20–29.
- Kimura, Y., Saito, R., Tsujimoto, Y., Ono, Y., Nakaya, T., Shobugawa, Y., Sasaki, A., Oguma, T., Suzuki, H., 2011. Geodemographics profiling of influenza A and B virus infections in community neighborhoods in Japan. *BMC Infect. Dis.* 11, 36.
- Laskowski, M., Mostaco-Guidolin, L.C., Greer, A.L., Wu, J., Moghadas, S.M., 2011. The impact of demographic variables on disease spread: influenza in remote communities. *Sci. Rep.* 1, 105.
- Loeb, M.B., 2003. Community-acquired pneumonia in older people: the need for a broader perspective. *J. Am. Geriatr. Soc.* 51, 539–543.
- Longini Jr., I.M., Koopman, J.S., Monto, A.S., Fox, J.P., 1982. Estimating household and community transmission parameters for influenza. *Am. J. Epidemiol.* 115, 736–751.
- Lu, P.-J., Singleton, J.A., Euler, G.L., Williams, W.W., Bridges, C.B., 2013. Seasonal influenza vaccination coverage among adult populations in the United States, 2005–2011. *Am. J. Epidemiol.* 178, 1478–1487.
- Mabry, P.L., Olster, D.H., Morgan, G.D., Abrams, D.B., 2008. Interdisciplinarity and systems science to improve population health: a view from the NIH Office of behavioral and social sciences research. *Am. J. Prev. Med.* 35, S211–S224.
- Marathe, A., Lewis, B., Chen, J., Eubank, S., 2011. Sensitivity of household transmission to household contact structure and size. *PLoS ONE* 6, e22461.
- Molinari, N.A., Ortega-Sanchez, I.R., Messonnier, M.L., Thompson, W.W., Wortley, P.M., Weintraub, E., Bridges, C.B., 2007. The annual impact of seasonal influenza in the US: measuring disease burden and costs. *Vaccine* 25, 5086–5096.
- Mossong, J., Hens, N., Jit, M., Beutels, P., Auranen, K., Mikolajczyk, R., Massari, M., Salmaso, S., Tomba, G.S., Wallinga, J., Heijne, J., Sadkowska-Todys, M., Rosinska, M., Edmunds, W.J., 2008. Social contacts and mixing patterns relevant to the spread of infectious diseases. *PLoS Med* 5, 381–391.
- Principi, N., Esposito, S., Marchisio, P., Gasparini, R., Crovari, P., 2003. Socioeconomic impact of influenza on healthy children and their families. *Pediatr. Infect. Dis. J.* 22, S207–S210.
- Statistics Canada, 2005. Census public use microdata files—families file. In: 2001 Census of Canada. Industry Canada, Ottawa, Canada.
- Stroud, P., Del Valle, S., Sydoriak, S., Riese, J., Mniszewski, S., 2007. Spatial dynamics of pandemic influenza in a massive artificial society. *J. Artif. Soc. Soc. Simul.* 10, 9.